Immune Profiling Reveals the T-Cell Effect of Ocrelizumab in Early Relapsing-Remitting Multiple Sclerosis

Alexandra Garcia, Emilie Dugast, Sita Shah, Jérémy Morille, Christine Lebrun-Frenay, Eric Thouvenot, Jérôme de Sèze, Emmanuelle Le Page, Sandra Vukusic, Aude Maurousset, et al.

RESEARCH ARTICLE OPEN ACCESS

Immune Profiling Reveals the T-Cell Effect of Ocrelizumab in Early Relapsing-Remitting Multiple Sclerosis

Alexandra Garcia, MSc,* Emilie Dugast, PhD,* Sita Shah, PhD, Jérémy Morille, PhD, Christine Lebrun-Frenay, MD, PhD, Eric Thouvenot, MD, PhD, Jérôme De Sèze, MD, PhD, Emmanuelle Le Page, MD, Sandra Vukusic, MD, PhD, Aude Maurousset, MD, Eric Berger, MD, Olivier Casez, MD, Pierre Labauge, MD, Aurélie Ruet, MD, PhD, Catarina Raposo, PhD, Fabien Bakdache, PharmD, Régine Buffels, MD, Fabienne Le Frère, MSc, Arnaud Nicot, PhD, Sandrine Wiertlewski, MD, Pierre-Antoine Gourraud, PhD, MPH, Laureline Berthelot, PhD, and David Laplaud, MD, PhD

Correspondence
Dr. Laplaud
david.laplaud@univ-nantes.fr

Neurol Neuroimmunol Neuroinflamm 2023;10:e200091. doi:10.1212/NXI.0000000000200091

Abstract

Background and Objectives

Ocrelizumab (OCR), a humanized anti-CD20 monoclonal antibody, is highly efficient in patients with relapsing-remitting multiple sclerosis (RR-MS). We assessed early cellular immune profiles and their association with disease activity at treatment start and under therapy, which may provide new clues on the mechanisms of action of OCR and on the disease pathophysiology.

Methods

A first group of 42 patients with an early RR-MS, never exposed to disease-modifying therapy, was included in 11 centers participating to an ancillary study of the ENSEMBLE trial (NCT03085810) to evaluate the effectiveness and safety of OCR. The phenotypic immune profile was comprehensively assessed by multiparametric spectral flow cytometry at baseline and after 24 and 48 weeks of OCR treatment on cryopreserved peripheral blood mononuclear cells and analyzed in relation to disease clinical activity. A second group of 13 untreated patients with RR-MS was included for comparative analysis of peripheral blood and CSF. The transcriptomic profile was assessed by single-cell qPCRs of 96 genes of immunologic interest.

Results

Using an unbiased analysis, we found that OCR as an effect on 4 clusters of $CD4^+$ T cells: one corresponding to naive $CD4^+$ T cells was increased, the other clusters corresponded to effector memory (EM) $CD4^+CCR6^-$ T cells expressing homing and migration markers, 2 of them also expressing CCR5 and were decreased by the treatment. Of interest, one $CD8^+$ T-cell cluster was decreased by OCR corresponding to EM CCR5-expressing T cells with high expression of the brain homing markers CD49d and CD11a and correlated with the time elapsed since the last relapse. These EM $CD8^+CCR5^+$ T cells were enriched in the CSF of patients with RR-MS and corresponded to activated and cytotoxic cells.

*These authors contributed equally to this work.

From the CHU Nantes (A.G., E.D., S.S., J.M., A.N., S.W., P.-A.G., L.B., D.L.), Nantes Université, INSERM UMR1064, Center for Research in Transplantation and Translational Immunology (CR2TI); CRCSEP (C.L.-F.), CHU de Nice Pasteur 2, Université Nice Côte d'Azur UR2CA URRIS; Service de Neurologie (E.T.), CHU de Nîmes, Institut de Génomique Fonctionnelle, Université de Montpellier, CNRS, INSERM; Service de Neurologie et Centre d'Investigation Clinique (J.D.S.), CHU de Strasbourg; Service de Neurologie (E.L.P.), CHU Pontchaillou, Rennes; Université de Lyon (S.V.), Université Claude Bernard Lyon 1; Service de Neurologie (S.V.), sclérose en plaques, pathologies de la Myéline et Neuro-inflammation, Hôpital Neurologique Pierre Wertheimer, Hospices Civils de Lyon, Bron; Observatoire Français de la Sclérose en Plaques (S.V.), Centre de Recherche en Neurosciences de Lyon; EUGENE DEVIC EDMUS Foundation Against Multiple sclerosis (S.V.), state-approved Foundation, Bron; Service de Neurologie (A.M.), CHU Bretonneau, Tours; Service de Neurologie (E.B.), CHU de Besançon; Service de Neurologie (O.C.), CHU de Grenoble; Service de Neurologie (P.L.), CHU de Montpellier, Montpellier; Service de Neurologie (A.R.), CHU de Bordeaux; Université de Bordeaux (A.R.), INSERM, Neurocentre Magendie; F. Hoffmann-La Roche Ltd (C.R., F.B., R.B.) CIC INSERM 1413 (F.L.F., S.W., D.L.), Nantes; CHU Nantes (S.W., D.L.), Nantes Université, Service de Neurologie; and CHU Nantes (P.-A.G.), Nantes Université, Clinique des données, France.

Go to Neurology.org/NN for full disclosures. Funding information is provided at the end of the article.

The Article Processing Charge was funded by CHU Nantes.

Glossary

ANOVA = analysis of variance; **ADCC** = antibody-dependent cell-mediated cytotoxicity; **BBB** = blood-brain barrier; **CCR** = C-C chemokine receptor type; **CCL** = C-C motif ligand; **CIS** = clinically isolated syndrome; **CM** = central memory; **EAE** = experimental autoimmune encephalomyelitis; **EM** = effector memory; **EOMES** = *Eomesodermin*; **FACS** = fluorescence-activated cell sorting; **FMO** = fluorescence minus one; **GZMB/K** = granzym B or K; **IFC** = integrated fluidic circuit; **LFA1** = lymphocyte function associated antigen 1; **MAIT** = mucosal-associated invariant T; **MS** = multiple sclerosis; **NK** = natural killer; **NMOSD** = neuromyelitis optica spectrum disorder; **OCR** = ocrelizumab; **OIND** = other inflammatory neurologic diseases; **PBMC** = peripheral blood mononuclear cell; **PRF1** = perforin 1; **qPCR** = quantitative PCR; **RR** = relapsing-remitting; **RPMI** = Roswell Park Memorial Institute medium; **SOM** = self-organizing map; **TBET** = T-box expressed in T cells; **t-SNE CUDA** = t-Distributed Stochastic Neighbor Embedding Compute Unified Device Architecture; **VLA4** = very late antigen-4.

Discussion

Our study provides novel insights into the mode of action of anti-CD20, pointing toward the role of EM T cells, particularly a subset of CD8 T cells expressing CCR5.

T cells have been initially thought to be central in multiple sclerosis (MS) process based on experimental autoimmune encephalomyelitis (EAE) findings, its animal model. However, B cell–depleting therapies such as rituximab, ofatumumab, and ocrelizumab (OCR) have proven their high efficacy for the treatment of MS both in randomized clinical trials and in observational studies, pointing out the central role of B cells in the disease process.[1-3] Nevertheless, their specific mechanisms of action are not fully understood yet. By contrast to the previous hypothesis on the efficacy of these treatments based on an effect on production of autoantibodies, newer evidence points more in the direction of a modified interaction of B cells with T cells and other parts of the immune system. Although B cells are the precursors of antibody-producing cells, they also have several main functions, including antigen presentation to T cells and cytokine secretion.[4,5]

In MS, B cells are found in the meninges of some patients with secondary progressive disease. They form aggregates of B and T cells associated with more severe disease[6] and cortical demyelination.[7] Moreover, it has been previously shown that B cells from patients with MS secrete more proinflammatory cytokines than their counterparts in healthy individuals.[8] Antigen presentation and cytokine secretion by B cells also induced an enhanced autoproliferation of B and T cells in patients with MS compared with healthy controls. They favored clonal selection of T cells with brain homing properties, which are being found in the lesions of patients with MS.[9] In this work, the anti-CD20 monoclonal antibody rituximab decreased autoproliferation of T cells. Taken together, it can be hypothesized that B-cell depletion may influence the fate of T cells and/or modify their phenotype in the periphery. Another potent mechanism of action may come from the depletion of a rare subset of T cells expressing CD20. These T cells are more frequently effector memory (EM) cells with proinflammatory properties,[10-13] more activated with better capabilities to transmigrate across the blood-brain barrier (BBB),[14,15] and may also be involved in the disease process.

To unravel the mechanisms of action of B-cell depletion and their consequences on the T-cell compartment, we took advantage of a cohort of treatment-naive patients with early relapsing-remitting (RR) MS enrolled in the multicenter ENSEMBLE study (NCT03085810) and treated with OCR every 6 months. Patients were sampled at baseline and 24 and 48 weeks after treatment started. We performed spectral flow cytometry covering 25 different markers at each time to deeply study the consequence of B-cell depletion on T cells. Finally, we confirmed our initial findings in the second cohort of untreated patients. We compared CSF and blood cells for their transcriptomic profile in a single-cell quantitative PCR (qPCR) analysis.

Methods

Samples

In this study, we investigated 3 groups of patients who provided informed consent to participate in this study in compliance with the Declaration of Helsinki and fulfill the eligibility criteria according to the McDonald 2010 criteria.[16] Group 1 consisted of 42 treatment-naive patients with RR-MS treated with OCR in the multicenter, open-label phase 3b ENSEMBLE study. All patients included have a definite diagnosis of RR-MS, a disease duration of less than or equal to 3 years, signs of clinical (i.e., relapse) or radiologic activity in the last 12 months, and an Expanded Disability Status Scale score of ≤3.5 at baseline. Blood sampling was performed at baseline and 24 and 48 weeks after starting OCR. Peripheral blood mononuclear cells (PBMCs) were isolated and frozen in liquid nitrogen at the Biological Resource Center of each participating center and sent to CHU de Nantes for a longitudinal spectral flow cytometry analysis.

Group 2 consisted of 12 blood and 3 CSF samples from untreated patients with RR-MS obtained from the MS center (CRC-SEP). Patients did not receive any disease-modifying drug for at least 6 months before sampling. CSF sampling was performed at the first clinical demyelinating event. PBMCs

Table 1 Clinical and Demographic Patient Characteristics at Baseline

	Group 1 MS (blood n = 42)	Group 2 MS (blood n = 13; CSF n = 3)	Group 3 OIND (blood n = 14; CSF n = 3)
Age (y)[a]	31.2 (8.0)	31.3 (9.9); 27.6 (11.6)	35.9 (11.2); 30 (7.9)
Female/male, n (%)	32 (76%)/10 (24%)	10 (76%)/3 (24%); 3 (100%)/0 (0%)	9 (64%)/5 (36%); 2 (67%)/1 (33%)
Time since the 1st symptom (mo)	14.28 (10.24)	55.1 (71.4); 0.47 (0.46)[b]	—
EDSS score[a]	1.54 (1.11)	1.18 (0.8); 1.33(1.15)[b]	—
% with gadolinium+	61.9	0[b]	—
NMOSD, n	—	—	8; 1
CIS[c]**, n**	—	—	5; 1
Viral meningoencephalitis, n	—	—	1; 1

Abbreviations: CIS = clinically isolated syndrome; EDSS = Expanded Disability Status Scale; NMOSD = neuromyelitis optica spectrum disorder; OIND = other inflammatory neurologic diseases.
[a] Mean with (SD).
[b] Missing data for 2 individuals.
[c] With lack of dissemination in space criteria (optic neuritis or myelitis without brain lesions), based on the McDonald 2010 criteria.

were isolated and frozen in liquid nitrogen for transcriptomic study. Fresh CSF cells were directly stained and sorted by flow cytometry cell sorting for transcriptomic study. Paired blood and CSF samples were obtained for 3 patients with MS.

Group 3 consisted of 14 blood samples from patients with other inflammatory neurologic diseases (OIND) of the CNS, including 8 patients with neuromyelitis optica spectrum disorder (NMOSD), 5 with clinically isolated syndrome (CIS) with lack of dissemination in space criteria (optic neuritis or myelitis without brain lesions), and 1 with viral meningoencephalitis. Three CSF samples from these patients (1 with NMOSD, 1 with CIS, and 1 with viral meningoencephalitis) were analyzed. PBMCs were isolated and frozen in liquid nitrogen for transcriptomic study. Fresh CSF cells were directly stained and sorted by flow cytometry cell sorting. The clinical and demographic characteristics of the 3 groups are summarized in Table 1.

Standard Protocol Approvals, Registrations, and Patient Consents

The relevant institutional review boards/ethics committees approved the trial protocols: Comité de Protection des Personnes for ENSEMBLE study (NCT03085810) and Agence de Biomédecine (ABM PFS13-003 Collection sclérose en plaques). All donors provided written informed consent in compliance with the Declaration of Helsinki.

T-Cell Profiling by Spectral Flow Cytometry

PBMCs were isolated using a standard Ficoll gradient according to the manufacturer's instructions (Eurobio) and frozen. After thawing, PBMCs (1.10^6 cells) were stained with the 2 T-cell panels: panel 1 with 15 extracellular markers and panel 2 with 14 extra-and intracellular markers listed in eTable 1A, links.lww.com/NXI/A802. The viability staining with the LIVE/DEAD™ Fixable Blue Dead Cell Stain Kit (Invitrogen) was performed at 4°C for 20 minutes. Then, the staining with the 2 panels of antibodies was performed at 4°C in staining buffer. The antibodies were added in sequential steps. First, C-C chemokine receptor type 7 (CCR7) was stained for 10 minutes, and then, other antibodies targeting chemokines were added for 10 minutes. Finally, extracellular markers were stained for 20 minutes. For panel 2, a permeabilization and fixation step (eBioscience FoxP3/TF staining buffer set) was performed after extracellular staining for 45 minutes at room temperature, and then, intracellular markers were stained for 30 minutes at room temperature. PBMCs were analyzed at baseline, 24 weeks, and 48 weeks of OCR treatment, using an Aurora 5-laser spectral flow cytometer (Cytek Biosciences). After individual titration of each antibody, a deconvolution matrix was set up, and a quality control procedure was performed prior to each data acquisition according to Cytek recommendations.

High-Dimensional Data Analysis of Flow Cytometry Data

Supervised analyses were performed using FlowJo (BD bioscience). The unsupervised t-Distributed Stochastic Neighbor Embedding Compute Unified Device Architecture (t-SNE CUDA) algorithm for dimensional reduction followed by Flow cytometry Self-Organizing Map (FlowSOM) analysis was performed on OMIQ (omiq.ai/). Flow cytometry standard files were first cleaned using FlowJo, and analyzed cells were gated on morphology followed by Singlet side scatter, Singlet forward scatter, and living lymphoid cells. At this stage, 9 patients were excluded from the analysis due to the lack of cells for at least 1 of the 3 time points. CD4 and CD8 T-cell subsets were analyzed separately. t-SNE CUDA analysis was performed using equal sampling of 1.10^4 cells from each time point, with 1,000 iterations, a perplexity of 30, and a theta of 0.5. The resulting t-SNE CUDA maps were fed into the FlowSOM clustering algorithm. A new self-organizing map (SOM) was generated using hierarchical consensus clustering on the t-SNE axes for each cell subset.

Figure 1 Overview of Spectral Flow Cytometry Analysis of Lymphocyte Subsets of Patients With MS Treated With Ocrelizumab

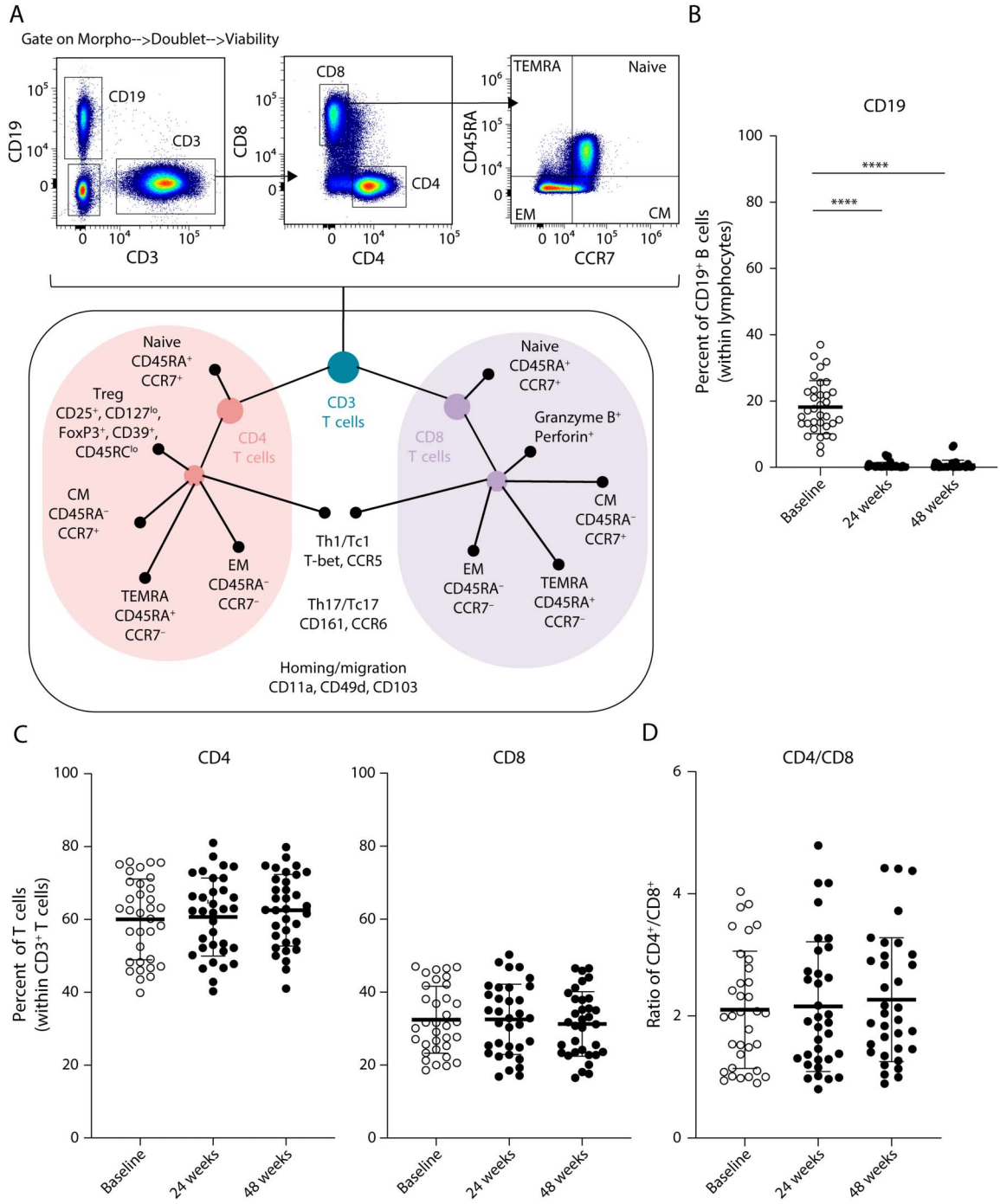

(A) Representation of the lymphocyte subsets and their associated markers, with an example of gating strategy on main immune cell populations at baseline. The gating strategy is shown after the exclusion of dead cells and doublets. B cells are gated on $CD19^+CD3^-$; $CD4^+$ lymphocytes are $CD3^+CD4^+$; $CD8^+$ lymphocytes are $CD3^+CD8^+$. The $CD4^+$ and $CD8^+$ T cells are also divided into naive cells: $CD45RA^+CCR7^+$, effector memory (EM) cells: $CD45RA^-CCR7^-$, central memory (CM) cells: $CD45RA^-CCR7^+$, and terminally differentiated effector memory cells re-expressing CD45RA (TEMRA): $CD45RA^+CCR7^-$. (B) Frequency (%) of $CD19^+$ B-cell subsets within lymphocytes at baseline (white) and after 24 and 48 weeks of OCR (black) (baseline 18.2% ± 8%, 48 weeks 0.7% ± 1.5%). (C) Frequency (%) of $CD4^+$ T cells (baseline 60.1% ± 11.1%, 48 weeks 62.5% ± 9.8%) and $CD8^+$ T cells (baseline 32.4% ± 9.2%, 48 weeks 31.3% ± 8.9%) at baseline (white) and 24 and 48 weeks of OCR treatment (black). (D) Ratio on CD4/CD8 T-cell subsets at baseline (white) and 24 and 48 weeks of OCR treatment (black). One-way ANOVA with correction by Tukey multiple comparison test was used (B–D). ****$p < 0.0001$ (mean with SD) (n = 32). MS = multiple sclerosis; OCR = ocrelizumab.

Cytotoxic Assay

PBMCs were isolated using a standard Ficoll gradient and stained with labeled antibodies listed in eTable1C, links.lww.com/NXI/A802. EM $CD8^+CCR5^+$ cells: $CD3^+CD8^+CCR5^+CCR7^-CD45RA^-CD20^-CD56^-$; B cells: $CD3^-CD20^+CD56^-$; and NK cells: $CD3^-CD20^-CD56^+$ were sorted using

the BD ARIA-FACS II cell sorter (Fluorescence-activated cell sorting). The purity of sorted cells from PBMCs was always above 80%. Sorted cells were cultured overnight in complete Roswell Park Memorial Institute medium (RPMI) medium with 200 U/mL IL2 (Miltenyi Biotec) in a round-bottom 96-well plate. Cells were then harvested, and EM $CD8^+CCR5^+$ and B cells were stained with CSFE (Invitrogen). Natural killer (NK) cells were added to the cell culture at an effector-to-target ratio of 5:1. Finally, OCR or control isotype was added to the cell culture at 0.1 μg/mL. After 4 hours, cells were stained with TO-PRO-3-iodide (Invitrogen) at 0.5 μM and immediately analyzed by flow cytometry. The background of TO-PRO-3-iodide staining was obtained by incubating the target cells with medium alone and the maximum staining by incubating the target cells with detergent.

Cell Sorting and Capture of Single Cells and Targeted Gene Preamplification

PBMCs were isolated using a standard Ficoll gradient and frozen until used for the second cohort of patients. Cells were thawed and stained with labeled antibodies against listed in eTable 1B, links.lww.com/NXI/A802. Fresh CSF samples were centrifuged for 10 minutes at 300*g*, and the cells were directly stained with the same antibody mix as for PBMCs. Live non–mucosal-associated invariant T (MAIT) cells and memory CD8 T cells ($CD3^+CD8^+CD45RA^-Vα7.2^-DAPI^-$) were sorted using the BD ARIA-FACS II cell sorter (BD Biosciences). The purity of sorted cells was always greater than 96%. Each single cell was isolated using the Fluidigm C1 system and C1 integrated fluidic circuits (IFC_5–10 μm). The C1 experiments were performed according to the manufacturer's instructions. Briefly, sorted live $CD3^+CD8^+CD45RA$ $Vα7.2^-$ cells were resuspended at 330,000 PBMC/mL of culture medium (RPMI1640, 10% fetal bovine serum, penicillin-streptomycin, and glutamine). As there were few CSF cells, they were resuspended in the minimal volume that could be loaded in the C1 chip corresponding to 6 μL. The C1 IFCs were primed, and cells were loaded into the IFCs using the Fluidigm C1 device. The chip was then imaged to confirm the single-cell capture in each well (wells with 2 or more cells were excluded). Following cell loading, the lysis final mix, reverse transcription final mix, and preamp final mix were prepared using the Single Cell-to-CT Kit (Ambion–Thermo Fisher Scientific). The preamp final mix contained a pool of 96 TaqMan probes (Thermo Fisher Scientific) at a concentration of 180 nM (eTable 2, links.lww.com/NXI/A802). All mixes were loaded on the IFCs, and the preamplified products were harvested the next morning.

Single-Cell Quantitative PCR

Following the C1 sample harvesting, we performed the first qPCR on a StepOnePlus instrument (Thermo Fisher Scientific) to confirm the presence of $CD8^+$ T cells using the CD8 TaqMan probe. The gene expression analysis of the preamplified amplicons was then performed with a 96.96 Dynamic Array IFC using the Biomark HD device allowing analysis of 96 genes using the TaqMan probe in 96 single cells simultaneously. The Biomark experiments were performed according to the manufacturer's recommendations.

Single-Cell Data Processing and Visualization

Ct values obtained from the Biomark System were converted into Log2Ex corresponding to the relative expression level obtained by subtracting the Ct value to the baseline (limit of detection) fixed at 28. We performed our analysis without normalization on an endogenous gene as we analyzed single cells. We excluded cells in which the CD3 and CD8 genes were not detected and those that expressed the CD4 gene. We also excluded cells that expressed less than 15 genes. Gene expression analyses from single cells were performed using RStudio software with the Fluidigm package and the Seurat package.

Statistical Analysis

All statistical supervised analyses were performed using GraphPad Prism 7, and unsupervised analyses were performed on OMIQ software (omiq.ai/), excel, and FaDA software (shiny-bird.univ-nantes.fr/app/Fada). For cohort 1, one-way analysis of variance (ANOVA) with correction by Tukey multiple comparison test and Bonferroni multiple test corrections were used as appropriate for the $CD4^+$ and $CD8^+$ T-cell part. One-way ANOVA with correction by Geisser-Greenhouse, Friedman test with Dunn correction, and Fisher exact test were used for the $CD3^+CD20^+$ part. For cohorts 2 and 3, the χ^2 test, Wilcoxon rank-sum test, Fisher exact test, unpaired *t* test, and *p* value corrections using Bonferroni or Benjamin and Hochberg methods were performed for the blood and CSF comparison part. The used test was annotated in the figure legend. Values are presented as mean ± SD. *p* Values were presented with * indicated as follows: $^*p \leq 0.05$, $^{**}p \leq 0.01$, $^{***}p \leq 0.001$, and $^{****}p \leq 0.0001$.

Data Availability

All raw data are available on reasonable request to the corresponding author.

Results

Identification of Lymphocyte Subsets

Using spectral flow cytometry, we investigated the effect of OCR treatment on lymphocytes from treatment-naive patients with RR-MS at baseline, 24 weeks, and 48 weeks of treatment. With our 2 antibody panels, we were able to cover the main T-cell populations. Thus, we looked at the naive and memory phenotypes (CD45RA and CCR7), the Th1/Tc1 cells (CCR5, T-bet, perforin, and granzyme B), the Th17/Tc17 cells (CCR6 and CD161), and the regulatory T cells (Treg: CD25, CD127, FoxP3, CD39, and CD45RC) (Figure 1A). For all these cell subsets, we looked at homing or migratory markers (CD49d and CD11a).

As expected, the total $CD19^+$ B-cell frequency and count (Figure 1B, eFigure 1A, links.lww.com/NXI/A802) were strongly reduced after OCR treatment. On the other hand,

Figure 2 CD4+ and CD8+ T-Cell Clusters Modified by Ocrelizumab

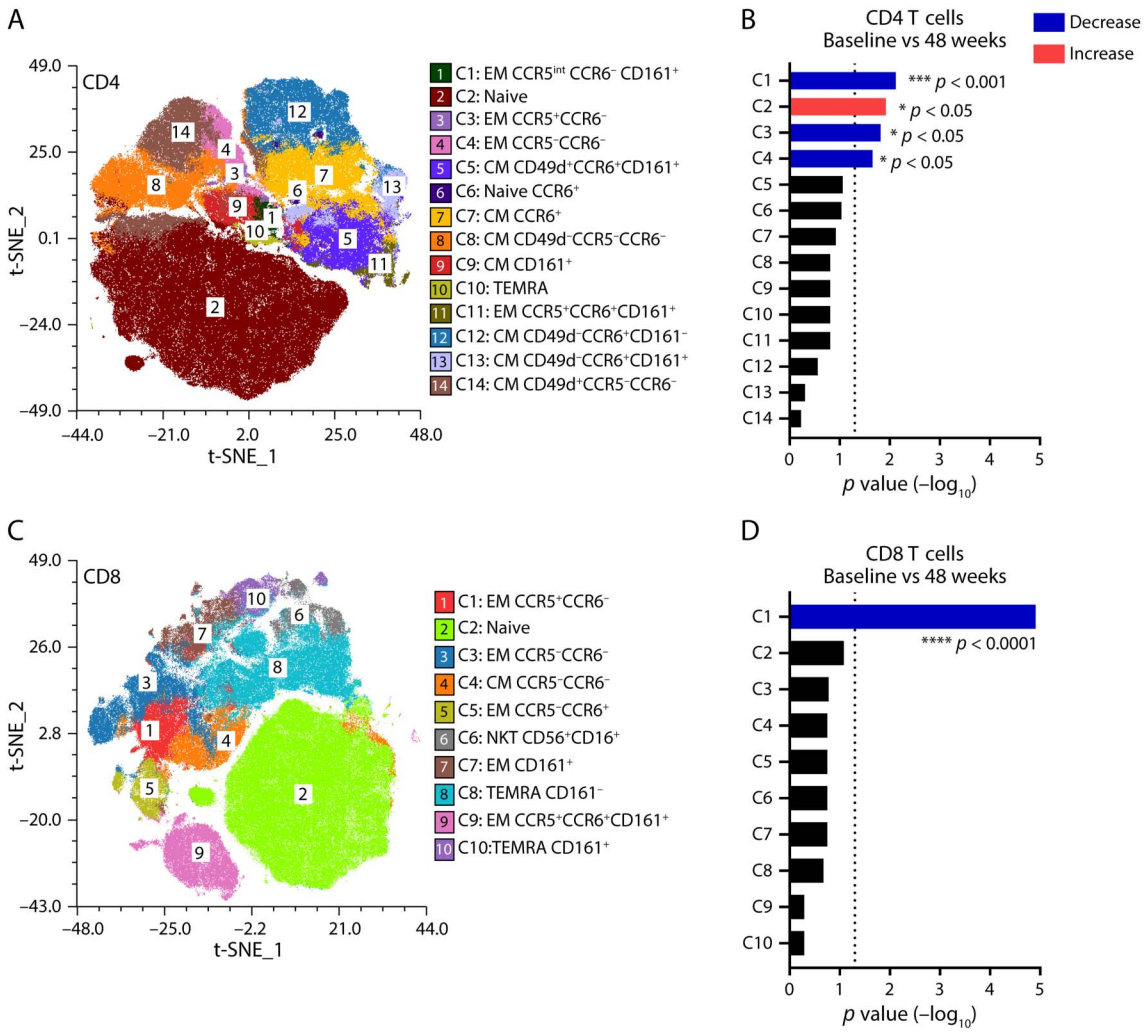

(A and C) t-SNE CUDA projections of $CD4^+$ (A) or $CD8^+$ (C) T-cell clusters identified by FlowSOM meta-clustering (1×10^4 cells/patient/time point). Fourteen clusters were identified for the $CD4^+$ T cells, and 10 clusters were identified for the $CD8^+$ T cells. (B and D) Representation of $CD4^+$ (B) and $CD8^+$ (D) T cells adjusted *p* value of the Bonferroni multiple tests used to compare each cluster at baseline and after 48 weeks of OCR treatment; in blue, the clusters that are decreased, and in red, the cluster that is increased. Unsupervised analyses were performed on OMIQ (omiq.ai/) (A and B). The Bonferroni multiple test correction was used (C and D). *$p < 0.05$, ***$p < 0.001$, and ****$p < 0.0001$ (n = 32). SOM = self-organizing map; t-SNE CUDA = t-Distributed Stochastic Neighbor Embedding Compute Unified Device Architecture.

no significant difference was observed in the frequency and count of $CD4^+$ and $CD8^+$ T cells (Figure 1C, eFigure 1, B–C, links.lww.com/NXI/A802) and the $CD4^+/CD8^+$ T-cell ratio (Figure 1D).

Ocrelizumab Did Not Induce Any Modification of Regulatory T-Cell Subsets

To look further, we applied high-dimensional flow cytometry unsupervised analysis to investigate whether the $CD4^+$ T-cell and $CD8^+$ T-cell subsets were affected by OCR treatment. We thus used the t-SNE CUDA algorithm for dimensional reduction followed by FlowSOM unsupervised clustering (eFigure 2, A–D, links.lww.com/NXI/A802). We performed the analysis with antibody panel 2, allowing us to identify 8 clusters of $CD4^+$ T cells and 10 clusters of $CD8^+$ T cells, including regulatory subsets (eTable 3, links.lww.com/NXI/A802). We did not observe any modification of each marker's frequency, abundance, or expression level in all the clusters after OCR treatment (eFigure 2, E–F, links.lww.com/NXI/A802).

Ocrelizumab Induced a Decrease of Some Effector Memory $CD4^+$ T Cells

We identified, using the same methodology, 14 $CD4^+$ T-cell clusters and 10 $CD8^+$ T-cell clusters (eTable 3, links.lww.com/NXI/A802) with antibody panel 1. Concerning the $CD4^+$ part, we showed that OCR resulted in significant modification of the frequency of 4 $CD4^+$ T-cell clusters (Figure 2, A and B). Among them, the frequency of the naive $CD4^+$ T-cell cluster (C2: $CD45RA^+CCR7^+$) increased, and in parallel, the frequencies of 3 other $CD4^+$ T-cell clusters (C1: EM $CCR5^{int}CCR6^-C161^+$; C3: EM $CCR5^+CCR6^+$; and C4: EM $CCR5^+CCR6^-$) decreased after 1 year of OCR treatment

Figure 3 Effect of Ocrelizumab on CD3+CD20+ T Cells

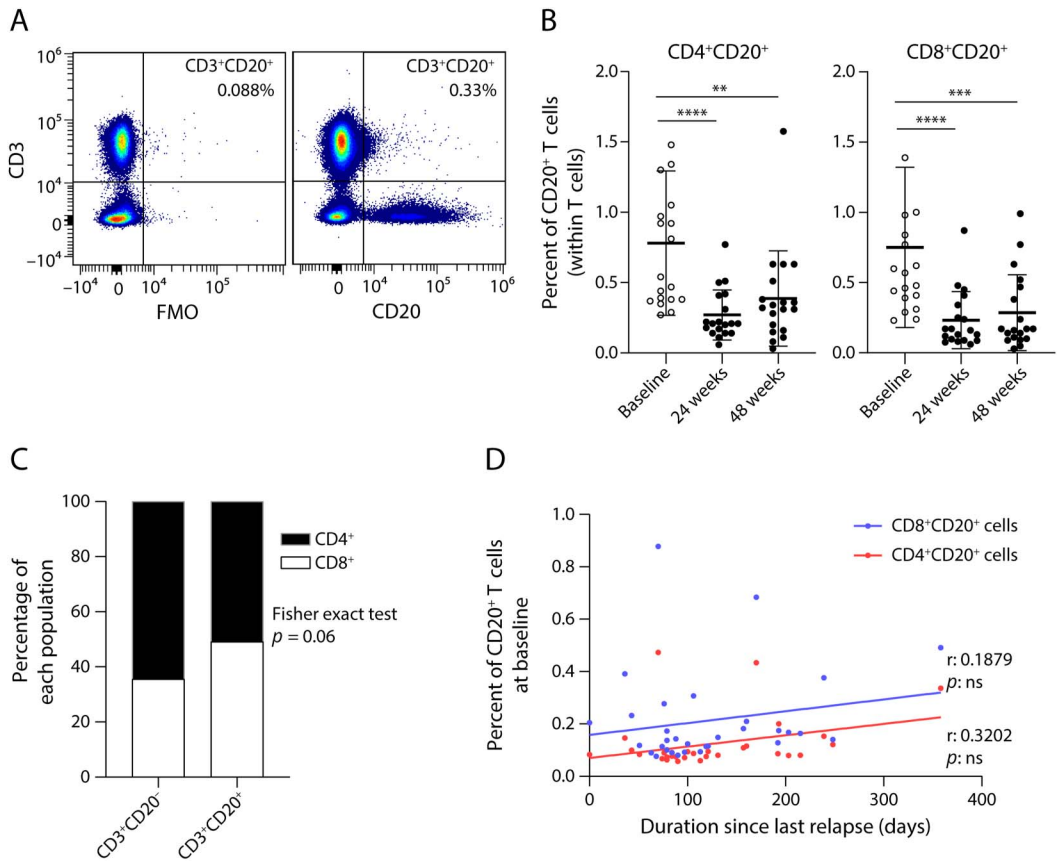

(A) Example for 1 representative patient of gating strategy on $CD3^+CD20^+$ T cells and FMO (without CD20 marker). (B) Frequency (%) of $CD4^+CD20^+$ and $CD8^+CD20^+$ T-cell subsets within lymphocytes at baseline (white) and after 24 and 48 weeks of OCR treatment (black). $CD4^+CD20^+$: baseline 0.78% ± 0.51%, 48 weeks 0.38% ± 0.33%; $CD8^+$ $CD20^+$: baseline 0.75% ± 0.57%, 48 weeks 0.28% ± 0.27%. (C) Proportion (%) of $CD8^+$ T cells (white) or $CD4^+$ T cells (black) within $CD3^+CD20^-$ or $CD3^+CD20^+$ T cells at baseline. (D) Correlation between the frequency of $CD4^+CD20^+$ (red) or $CD8^+$ $CD20^+$ (blue) T cells at baseline and the duration since the last relapse (days). Friedman test with Dunn correction (B), Fisher exact test (C) and linear regression, and Spearman *r* (D) were used. $^{**}p < 0.01$, $^{***}p < 0.001$, and $^{****}p < 0.0001$ (mean with SD) (n = 20) FMO = Fluorescence Minus One.

(eFigure 3A, links.lww.com/NXI/A802). Of interest, all these 3 clusters shared an overexpression of the migration markers CD11a and CD49d, indicating their ability to transmigrate across the BBB (eFigure 3C, links.lww.com/NXI/A802). In addition, cluster C1 is associated with the expression of CD161 and may correspond to a CD4 subset of Th1 or Th17.1 cells.[17] A global decrease of Th1 cells is probable and confirmed by the decreased frequency of T-bet–expressing CD4 T cells during treatment (eFigure 4, links.lww.com/NXI/A802).

Ocrelizumab Induced a Decrease of an Effector Memory $CD8^+CCR5^+$ T-Cell Subset

Despite no modification in the $CD8^+$ T-cell global proportion, 1 $CD8^+$ T-cell cluster among the 10 identified (eTable 3, links.lww.com/NXI/A802) was significantly modified after OCR treatment (Figure 2, C and D). The frequency of $CD8^+$ T cells constituting this cluster (C1: EM $CCR5^+CCR6^-$) decreased after treatment and corresponded to an EM $CCR5^+$ subset (eFigure 3B, links.lww.com/NXI/A802). These cells expressed a high level of CD49d and CD11a homing and migratory markers. The global expression of markers was compared at baseline and after treatment, and no modification was observed, suggesting that OCR affected only the frequency but not the phenotype of these cells at least with the markers used here (eFigure 3D, links.lww.com/NXI/A802). The only other CD8 cluster expressing CCR5 (C9: EM $CCR5^+CCR6^+CD161^+$) was composed of $CD161^{high}$ T cells, likely corresponding to MAIT cells,[18] and was not modified by the treatment.

Ocrelizumab Depleted $CD3^+CD20^+$ T Cells and Indirectly Decreased EM $CD8^+CCR5^+$ and EM $CD4^+CCR6^-$ T Cells

A specific subset of T cells expressing CD20 at low level seems to be involved in the pathophysiology of MS.[10,11,14,15,19] We also investigated the effect of OCR on $CD3^+CD20^+$ T cells and their subsets $CD4^+CD20^+$ and $CD8^+CD20^+$ T cells (Figure 3A).

We showed that the frequency and count of these cells were very low in the circulation at baseline and were significantly decreased by OCR at 24 and 48 weeks (Figure 3B, eFigure 5A, links.lww.com/NXI/A802). In addition, there was a tendency for an increased proportion of $CD8^+$ T cells in the $CD3^+CD20^+$ compartment compared with $CD3^+CD20^-$

Figure 4 No Implication of CD20+ T Cells in the Decrease of EM T-Cell Clusters

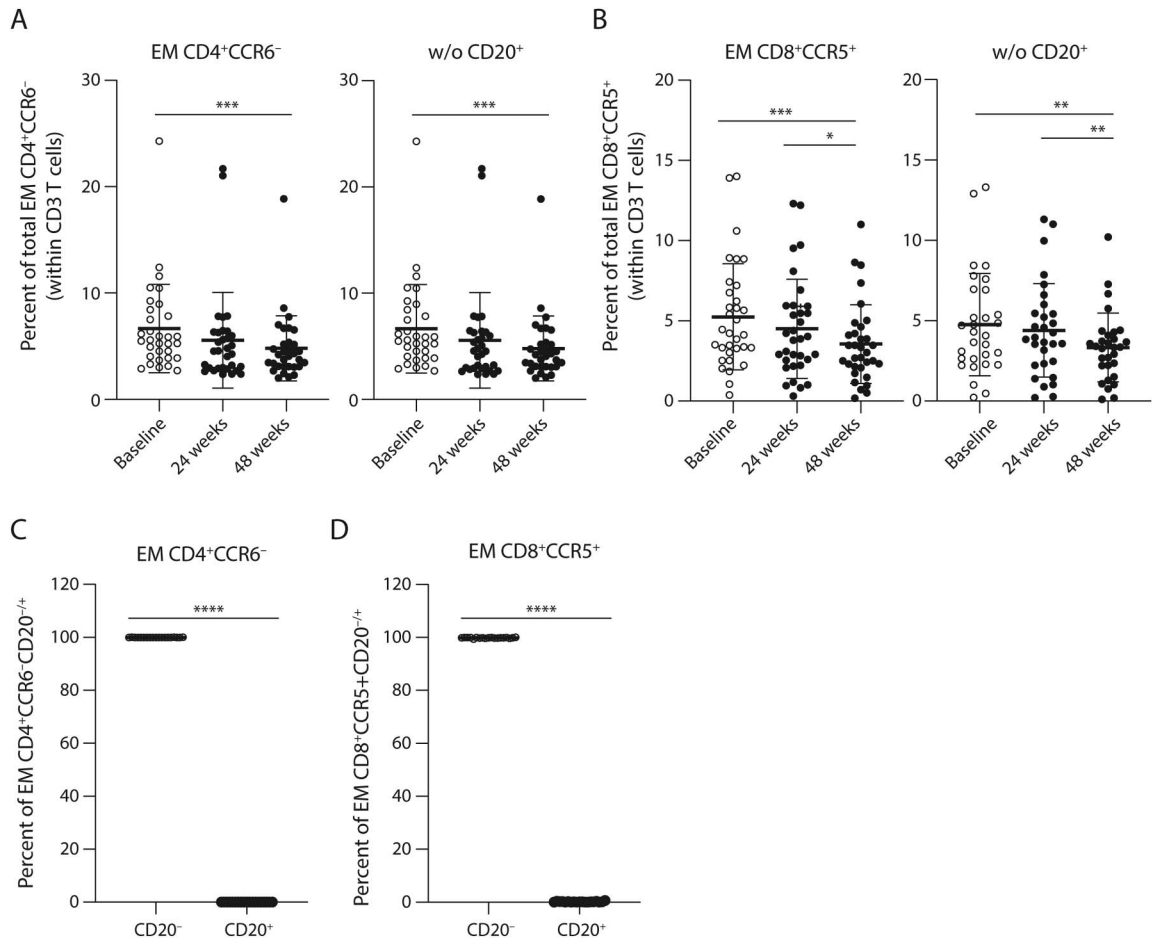

(A and B) Frequency (%) of EM $CD4^+CCR6^-$ T cells (corresponding to clusters C1, C2, and C4) (A) and EM $CD8^+CCR5^+$ (B) T cells (corresponding to cluster C1) within $CD3^+$ T cells and the same frequency with depletion of $CD20^+$ T cells at baseline (white) and 24 and 48 weeks of OCR treatment (black). (C and D) Frequency (%) of $CD4^+CCR6^-CD20^-$ or $CD20^+$ T cells (C) and EM $CD8^+CCR5^+$ $CD20^-$ or $CD20^+$ T cells (D). The Friedman test with Dunn correction (A and B) and the paired *t* test (C and D) were used. **p* < 0.05, ***p* < 0.01, ****p* < 0.001, and *****p* < 0.0001 (mean with SD) (n = 20). EM = effector memory.

T cells (Figure 3C). The phenotype at baseline of $CD4^+CD20^+$ and $CD8^+CD20^+$ T cells was different compared with their counterpart $CD20^-$ T cells with an increase of CCR5 and CCR6 frequency (eFigure 5B, links.lww.com/NXI/A802) and an overexpression of CD49d and CD11a in cells expressing CD20 (eFigure 5C, links.lww.com/NXI/A802). We found that $CD4^+CD20^+$ and $CD4^+CD20^-$ T cells have similar repartition in terms of naive, central memory (CM), EM, and terminally differentiated EM cells re-expressing CD45RA at baseline (eFigure 5, D–E, links.lww.com/NXI/A802). Concerning the $CD8^+CD20^+$ subset, we confirmed that the phenotype of these cells was significantly less naive but more CM and EM than $CD8^+CD20^-$ T cells (eFigure 5F, links.lww.com/NXI/A802). In addition, we were unable to establish a correlation between the time elapsed since the last relapse and the frequency of $CD4^+CD20^+$ and $CD8^+CD20^+$ T cells at baseline (Figure 3D).

Next, the question was to explore whether our previous observation that OCR reduced EM $CD4^+CCR6^-$ T cells (clusters C1, C2, and C4) and EM $CD8^+CCR5^+$ T cells (cluster C1) was due to a depletion of $CD20^+$ T cells or not. For that, we assessed the frequency of EM $CD4^+CCR6^-$ T cells and EM $CD8^+CCR5^+$ T cells under OCR and after exclusion of $CD20^+$ T cells (Figure 4, A and B). The results were similar, indicating that the depletion of $CD20^+$ T cells did not account for the effects observed due to their low frequency in EM $CD4^+CCR6^-$ (0.028 ± 0.023%) and EM $CD8^+CCR5^+$ (0.16 ± 0.16%) T cells (Figure 4, C and D). Moreover, antibody-dependent cell-mediated cytotoxicity (ADCC) cytotoxic assay revealed that OCR induced depletion of $CD20^+$ B cells by NK cells but not EM $CD8^+CCR5^+CD20^-$ T cells (eFigure 6, links.lww.com/NXI/A802), confirming a lack of the direct effect of OCR on these cells.

Frequency of EM $CD8^+CCR5^+$ T Cells Positively Correlates With the Activity of the Disease.

We explored a possible relationship between the frequency of the $CD4^+$ T-cell clusters (C1: EM $CCR5^{int}CCR6^-CD161^+$; C2: naive; C3: EM $CCR5^+CCR6^+$; and C4: EM $CCR5^-CCR6^-$) or the $CD8^+$ T-cell cluster (C1: EM $CD8^+CCR5^+$) at baseline and

Figure 5 Correlation Between CD4+ and CD8+ T-Cell Clusters and the Clinical Activity of the Disease

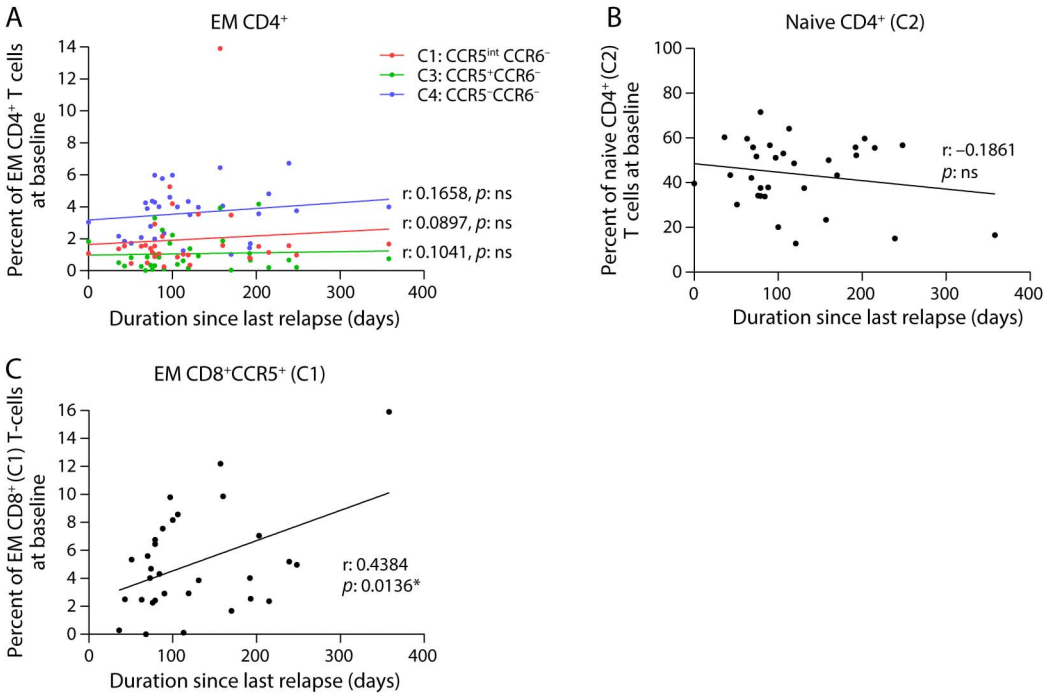

(A) Correlation between the frequency of EM CD4$^+$ T-cell clusters (C1: EM CCR5^{int}CCR6$^-$CD161$^+$ [red]; C3: EM CCR5$^+$CCR6$^-$ [green]; and C4: EM CCR5$^-$CCR6$^-$ [blue]) at baseline and the time elapsed since the last relapse (days) before the beginning of OCR treatment. (B) Correlation between the frequency of the naive CD4$^+$ T-cell cluster (C2) at baseline and the time elapsed since the last relapse (days) before the beginning of OCR treatment. (C) Correlation between the frequency of the CD8$^+$ T-cell cluster (C1: EM CD8$^+$CCR5$^+$) at baseline and the time elapsed since the last relapse (days) before the beginning of OCR treatment. Linear regression, Pearson *r* (A–C) was used. *$p < 0.05$, (n = 32). EM = effector memory; OCR = ocrelizumab.

modified by OCR and the clinical activity of the disease at baseline. We found that CD4$^+$ T-cell clusters were not correlated with clinical activity (Figure 5, A and B), whereas the CD8$^+$ T-cell cluster (C1) is the only cluster that positively correlated with the time since the last relapse ($r = 0.438$, $p = 0.0136$) (Figure 5C). This result indicates that the lower the frequency of circulating EM CD8$^+$CCR5$^+$ T cells, the more recent the relapse and strongly suggests a direct implication of this subset of cells at the peak of neuroinflammation.

CSF Compartment Is Enriched in EM CD8$^+$ T Cells Expressing CCR5

To explore this hypothesis, we studied memory CD8$^+$ T cells from the blood and CSF of patients with MS and OIND at the single-cell level, using a 96-gene qPCR array. We first combined all the single-cell qPCR data obtained from both blood and CSF samples of patients with RR-MS and compared the global molecular profile regarding the expression of up to 80 genes to identify a cell subset associated with the blood or CSF compartment in an unbiased way. Using the t-SNE algorithm for dimensionality reduction and K-means clusterization, we were able to divide all the cells into 5 clusters. Among these 5 clusters, in MS, cluster 2 was significantly associated with CSF cells, and cluster 3 was mainly composed of cells from the blood (Figure 6A). The heatmap summarized the genes that mostly influenced the cell clusterization (Figure 6B). These data uncovered the cells from cluster 2—associated to the CSF—were nearly the only ones to express the *CCR5* gene. We also showed that these cells expressed a high level of *granzyme A*, an intermediate level of *perforin*, the transcription factor Eomesodermin (*EOMES*), the chemokine C-C motif ligang 5 (*CCL5*), the resident/activation marker *CD69*, and the migratory markers Lymphocyte Function Associated antigen 1 (*LFA1*) and Very Late Antigen-4 (*VLA4*), suggesting that they harbor a peculiar cytotoxic profile with a potential T resident memory phenotype. Moreover, they expressed *granzyme K* at a high level, which has been recently associated with the ability of cells to cross the blood-brain barrier.[17] Moreover, when we looked at the number of CCR5$^+$ vs CCR5$^-$ cell repartition in the blood and the CSF, we show that the cells from the CSF were significantly enriched in CCR5$^+$ cells compared with cells from the blood compartment (43.59% in CSF vs 11.28% in blood, $p < 0.0001$) (Figure 6C).

Then, we compared the expression profile of the CCR5$^+$ CD8$^+$ T cells in the CSF with those of the peripheral blood (Figure 6D), and we did not find significant differences between the 2 compartments for cytokines. In contrast, *EOMES* gene expression, associated with the CD8$^+$ T-cell exhaustion and effector functions, was upregulated in the CSF compared with the blood CD8$^+$ CCR5$^+$ T cells. Of interest, none of the molecules associated with cell cytotoxicity were modified between CSF and blood. These results suggest rather an increased frequency of the cells in the CSF than a profound modification of their phenotype.

Figure 6 Identification of the CCR5+CD8+ T-Cell Subset in the CSF of Patients With MS

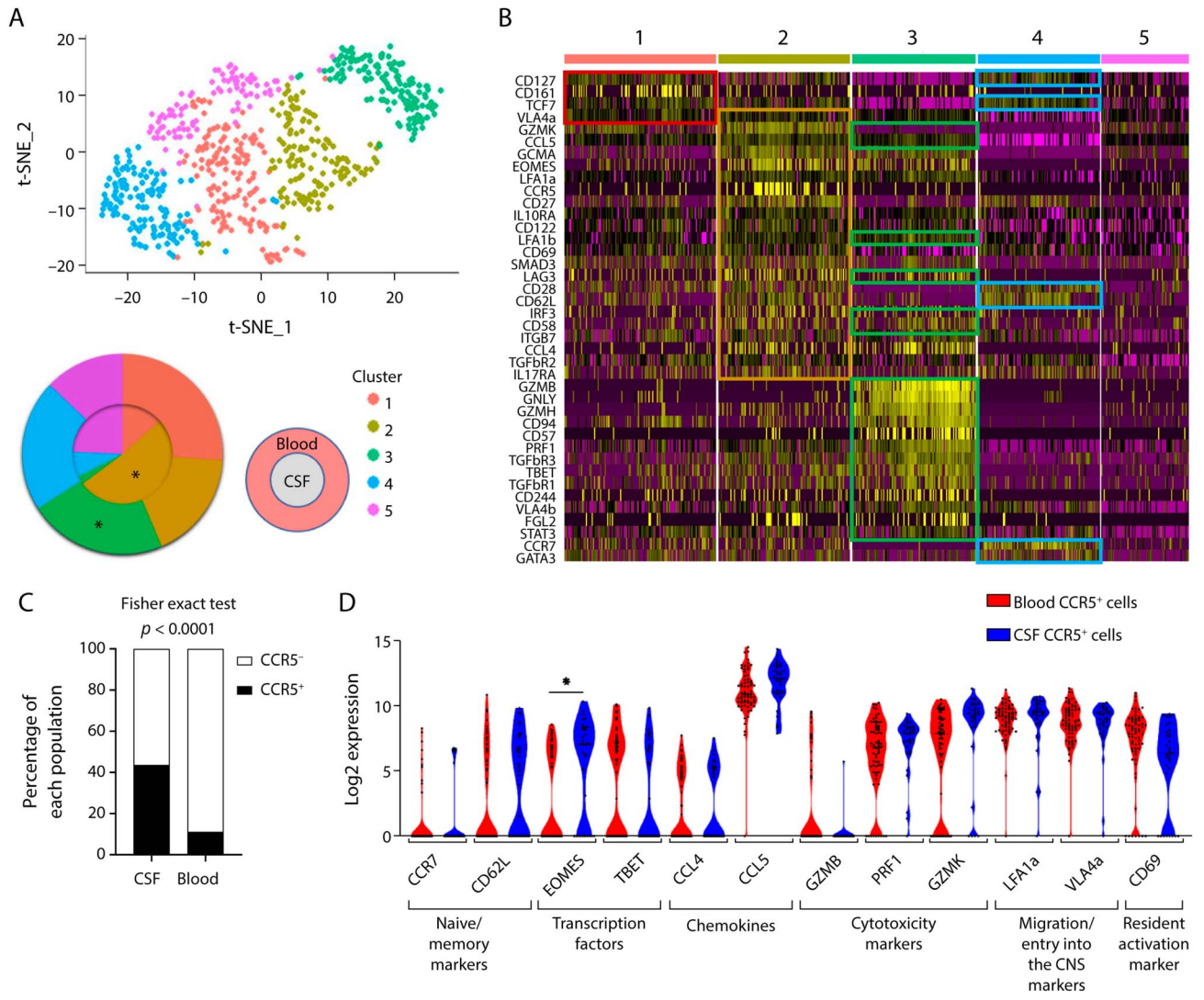

(A) t-SNE projection of transcriptomic data of blood and CSF single cells from patients with MS. Each dot corresponds to 1 single cell and is colored according to its cluster. Clustering is made using the K-means methods, and 5 clusters are defined from 1 to 5. The pie chart summarizes the cell proportions in each cluster. The inner circle represents cells from CSF, and the outer circle represents cells from the blood. Stars indicate when the proportion in the clusters is significantly higher in one group than the other. (B) Heatmap of the most significant genes defining the clusters with the blood and CSF single cells from patients with MS. Genes that are circled in each cluster are those that are significantly relevant to define the cluster. (C) Proportion (%) of $CCR5^+$ $CD8^+$ T cells (in black) and $CCR5^-$ $CD8^+$ T cells (in white) in the CSF or the blood of patients with MS. (D) Violin plots of the expression level of some relevant genes *CCR7, CD62L, EOMES, TBET, CCL4, CCL5, GZMB, PRF1, GZMK LFA1, VLA4A, and CD69* in $CCR5^+$ $CD8^+$ T cells from the blood compared with those from the CSF. The χ^2 test was performed to identify significant differences in proportion, and adjusted residues were calculated to define these differences between clusters (* mean statistically linked to the group) (A). The Wilcoxon rank-sum test, $p < 0.05$ (B), Fisher exact test (C), and unpaired *t* test and *p* value corrections using Bonferroni or Benjamin and Hochberg (BH) methods (D) were used. *$p < 0.05$, (blood n = 12; CSF n = 3). MS = multiple sclerosis.

To know whether the CSF profile of EM $CD8^+CCR5^+$ T cells was specific of patients with MS or rather tissue specific, we compared with the same methodology blood and CSF cells obtained from 14 patients with OIND (mainly NMOSD and CIS without brain lesions). The unsupervised analysis showed that the only cluster significantly associated with CSF was cluster A, composed of cells that do not express *CCR5* (eFigure 7, links.lww.com/NXI/A802). Cluster B, which is the one characterized by the *CCR5* expression, was equally distributed in blood and CSF cells. Altogether, these data suggest that the cluster of cells expressing *CCR5* and recruited in the CSF is MS specific.

Discussion

In this work, we had the opportunity to study the effect of OCR-induced B-cell depletion on peripheral T cells in a cohort of treatment-naive patients with RR-MS enrolled in a study at the beginning of their disease. The first significant observation is that B-cell depletion mainly affects CCR5-expressing T cells, especially in EM CD8 T cells, by indirectly decreasing their frequency in the peripheral blood, which was confirmed by cytotoxic assay. Of interest, this population also expressed markers of transmigration, and its frequency was increased in the CSF of patients with MS. The lower the

frequency of EM $CD8^+CCR5^+$ T cells in the blood, the shorter the time elapsed since the last relapse. At first sight, this result may be counterintuitive. The fact that a low percentage of $CD8^+CCR5^+$ T cells in the blood is associated with a recent relapse suggests the possibility of 2 hypotheses: the cells may be of suppressive function (such T cells with proinflammatory patterns have been recently highlighted with Kir^+CD8^+ T cells[20,21]), or as $CCR5^+$ T cells are increased in the CNS of patients,[22,23] they may belong to a peripheral reservoir that is mobilized during a neuroinflammatory attack. As the CCR5/CCL4-5 axis is a crucial driving force for T-cell entry into the CNS,[23] our observation of decreased EM $CD8^+CCR5^+$ T-cell subset in the periphery with disease activity is in agreement with the current notion that these cells are prone to migrate into the CNS and contribute to the peak of neuroinflammation.

Only very few studies focused on the implication of B-cell depletion on the T-cell compartment in MS. An increase in naive CD4 and CD8 T cells under treatment has been previously reported.[24] In primary progressive MS, it has been shown a significant increase of naive CD4 and CD8 T cells under OCR, together with a decrease of terminally differentiated CD4 T cells and of EM CD8 T cells. Although we confirm some of these findings[25] in our cohort of patients, we found that the effect of B-cell depletion is more complex. Indeed, it affects specific subsets of EM T cells in both compartments and mainly those expressing CCR5 and the homing markers CD49d and CD11a. These results are in accordance with studies pointing out the role of a subset of Th cells expressing CCR2 and CCR5 and associated with the activity of MS.[26,27] Indeed, 3 clusters of EM CD4 T cells with common features were decreased by OCR. C1 and C3 both expressed CCR5 and are close to an already described population of T cells associated with MS[26] expressing CCR2 and CCR5. These EM $CD4^+CCR6^-$ T cells may belong to a Th1 phenotype as confirmed by the decrease of T-bet–expressing CD4 T cells after OCR treatment.

Anti-CD20 therapy may also affect a small subset of T cells expressing CD20. $CD3^+CD20^+$ T cells have been shown to have a proinflammatory Th1/Tc1 phenotype and accumulate in the blood and CSF of patients with MS.[13] We confirm the proinflammatory phenotype of these subsets with properties of migration to the CNS as they express CD49d and CD11a. We confirm the recent findings that OCR significantly depletes these CD4 and CD8 subsets.[14,15] However, the effect of B-cell depletion on the frequency of the main subsets affected by OCR, including EM $CD8^+CCR5^+$ and EM $CD4^+CCR6^-$ T cells, seems to be independent of the depletion of these CD20-expressing T cells since when we exclude them from the general T-cell analysis, the results are identical. These results do not support recent findings showing that depletion of $CD20^+$ T cells by ofatumumab leads to a decrease in T cells able to transmigrate across a model of BBB.[15] There is no clear explanation for this discrepancy, but several differences can be made with our study like the number of patients included, the anteriority of immunosuppressant treatment, and the duration of the disease. However, it is difficult to draw definitive conclusions as the frequency of $CD3^+CD20^+$ T cells found in our study is in the low range compared with the literature, making difficult some correlations.[11,13,28,29]

To understand how the decrease of some subsets of T cells may affect the disease, we investigated the CSF and blood of patients with MS and OIND of the CNS at the single-cell level in sorted memory $CD8^+$ T cells. We demonstrate that EM $CD8^+CCR5^+$ T cells, those affected by OCR in the periphery, correspond to a subset of cells recruited in the CSF and specific of patients with MS. Indeed, CCR5 memory $CD8^+$ T cells represent up to 45% of the memory $CD8^+$ T cells found in the CSF and around 11% of the circulating memory $CD8^+$ T cells. CCR5 appears to be a marker of cells of interest in MS not only based on these findings but also because CCR5-expressing cells are numerous in the lesions of MS,[30] indicating a possible role in the lesion process, and because of the correlation of the frequency of these cells in the periphery and the advent of relapses. Hence, in EAE, the blocking of CCR5 by maraviroc, a specific antagonistic agent, alleviates the disease,[31] indicating the involvement of T cells expressing CCR5 in neuroinflammation. In addition, when comparing the phenotype of EM $CD8^+CCR5^+$ T cells, we found similarities across cells located in both the blood and the CSF, suggesting that these cells are activated in the periphery and that their differentiation is not happening in the CNS. We can hypothesize that these cells migrate in their fully differentiated phenotype. As IgG monoclonal antibodies have low permeability across the BBB,[32] these results suggest that the OCR effect on the reduction of EM $CD8^+CCR5^+$ T cells may occur mainly in the periphery. Because of that, we have reason to believe that OCR treatment depletes EM $CD8^+CCR5^+$ T cells in the periphery, thereby providing some beneficial effect on the activity of the disease.

Altogether, we show that the B cell–targeting, anti-CD20 therapy OCR indirectly affects the frequency of specific peripheral EM $CD8^+CCR5^+$ T cells and EM $CD4^+CCR6^-$ T cells, both being able to migrate to the CNS. Although we still have to determine how exactly OCR treatment affects the T-cell compartment, our study provides a way to explain one of the possible beneficial effects that OCR treatment has on MS clinical activity.

Acknowledgment

The authors thank the patients for their participation in the study and the biological resource center for biobanking (CHU Nantes, Hôtel Dieu, Centre de ressources biologiques [CRB], Nantes, F-44093, France [BRIF: BB-0033-00040]). The authors are also grateful to Nicolas Degauque for assistance with OMIQ analysis and Laurence Delbos (Head of CR2TI Cytometry and Cell Sorter Core Facility) for excellent assistance with spectral cytometry. OFSEP is supported by a grant provided by the French state and handled by the Agence Nationale de la Recherche, within the framework of the Investments for the Future Programme, under the reference ANR-10-COHO-002, by the EDMUS Foundation against MS, and by the ARSEP Foundation.

Study Funding

The study was granted by F. Hoffmann-La Roche Ltd. This study was also supported by the Association ANTARES and OFSEP and by the ARSEP Foundation.

Disclosure

E. Thouvenot declares consultancy and board membership from Novartis, BMS, Merck, Actelion, and Teva and grants from Novartis, Biogen, and Merck. E. Le Page declares research support from Teva and has received honoraria for lectures or consulting from Biogen Idec, Merck-Serono, Novartis, Sanofi-Aventis, Alexion, Roche, and Jansen. S. Vukusic declares board membership, consultancy, grants, and payment for lectures from BMS, Biogen, Merck, Novartis, Roche, Sanofi, and Janssen. A. Maurousset declares board membership from Alexion, Merck, and Novartis and expert testimony from Sanofi and Merck. E. Berger declares board membership from Biogen, Roche, and Novartis. O. Casez declares board membership from BMS, Merck, Novartis, and Roche and payment for manuscript preparation from Biogen, Novartis, Roche, and Sanofi. A. Ruet declares board membership and consultancy from Merck, Novartis, and Roche and grants from Bayer HealthCare, Biogen, Roche, and Sanofi. P.-A. Gourraud declares consultancy for AstraZeneca, Biogen, Boston Scientific, Cook, Edimark, Ellipses, Elsevier, Methodomics, Merck, Mérieux, Sanofi-Genzyme, and WeData. He has no prescription activity, neither drugs nor devices. S. Wiertlewski declares board membership from Biogen, Novartis, and Roche. F. Bakdache, C. Raposo, and R. Buffels are employees from Hoffmann-La Roche. D. Laplaud declares board membership, consultancy, and grants from Alexion, Actelion, BMS, Biogen, Merck, Novartis, Roche, and Sanofi. Go to Neurology.org/NN for full disclosures.

Publication History

Received by *Neurology: Neuroimmunology & Neuroinflammation* June 17, 2022. Accepted in final form December 12, 2022. Submitted and externally peer reviewed. The handling editor was Deputy Editor Scott S. Zamvil, MD, PhD, FAAN.

Appendix Authors

Name	Location	Contribution
Alexandra Garcia, MSc	CHU Nantes, Nantes Université, INSERM, Center for Research in Transplantation and Translational Immunology, France	Drafting/revision of the manuscript for content, including medical writing for content; major role in the acquisition of data; study concept or design; and analysis or interpretation of data
Emilie Dugast, PhD	CHU Nantes, Nantes Université, INSERM, Center for Research in Transplantation and Translational Immunology, France	Drafting/revision of the manuscript for content, including medical writing for content; major role in the acquisition of data; and analysis or interpretation of data
Sita Shah, PhD	CHU Nantes, Nantes Université, INSERM, Center for Research in Transplantation and Translational Immunology, France	Drafting/revision of the manuscript for content, including medical writing for content
Jérémy Morille, PhD	CHU Nantes, Nantes Université, INSERM, Center for Research in Transplantation and Translational Immunology, France	Drafting/revision of the manuscript for content, including medical writing for content
Christine Lebrun-Frenay, MD, PhD	CRCSEP, CHU de Nice Pasteur 2, Université Nice Côte d'Azur UR2CA URRIS, France	Drafting/revision of the manuscript for content, including medical writing for content
Eric Thouvenot, MD, PhD	Service de Neurologie, CHU de Nîmes, Nîmes, France, Institut de Génomique Fonctionnelle, Université de Montpellier, CNRS, INSERM, France	Drafting/revision of the manuscript for content, including medical writing for content
Jérôme De Sèze, MD, PhD	Service de Neurologie et Centre d'Investigation Clinique, CHU de Strasbourg, INSERM 1434, Strasbourg, France	Drafting/revision of the manuscript for content, including medical writing for content
Emmanuelle Le Page, MD	Service de Neurologie, CHU Pontchaillou, Rennes, France	Drafting/revision of the manuscript for content, including medical writing for content
Sandra Vukusic, MD, PhD	Université de Lyon, Université Claude Bernard Lyon 1, Lyon; Service de Neurologie, sclérose en plaques, pathologies de la myéline et neuro-inflammation, Hôpital Neurologique Pierre Wertheimer, Hospices Civils de Lyon, Bron; Observatoire Français de la Sclérose en Plaques, Centre de Recherche en Neurosciences de Lyon, INSERM 1028 et CNRS UMR 5292, Lyon; EUGENE DEVIC EDMUS Foundation against multiple sclerosis, state-approved foundation, Bron, France	Drafting/revision of the manuscript for content, including medical writing for content
Aude Maurousset, MD	Service de Neurologie, CHU Bretonneau, Tours, France	Drafting/revision of the manuscript for content, including medical writing for content
Eric Berger, MD	Service de Neurologie, CHU de Besançon, Besançon, France	Drafting/revision of the manuscript for content, including medical writing for content
Olivier Casez, MD	Service de Neurologie, CHU de Grenoble, Grenoble, France	Drafting/revision of the manuscript for content, including medical writing for content
Pierre Labauge, MD, PhD	Service de Neurologie, CHU de Montpellier, Montpellier, France	Drafting/revision of the manuscript for content, including medical writing for content

Appendix *(continued)*

Name	Location	Contribution
Aurélie Ruet, MD, PhD	Service de Neurologie, CHU de Bordeaux, Bordeaux, France; Université de Bordeaux, INSERM, Neurocentre Magendie, France	Drafting/revision of the manuscript for content, including medical writing for content
Catarina Raposo, PhD	F. Hoffmann-La Roche Ltd, France	Drafting/revision of the manuscript for content, including medical writing for content
Fabien Bakdache, PharmD	F. Hoffmann-La Roche Ltd, France	Drafting/revision of the manuscript for content, including medical writing for content
Régine Buffels, MD	F. Hoffmann-La Roche Ltd, France	Drafting/revision of the manuscript for content, including medical writing for content, and study concept or design
Fabienne Le Frère, MSc	CIC INSERM 1413, Nantes, France	Drafting/revision of the manuscript for content, including medical writing for content
Arnaud Nicot, PhD	CHU Nantes, Nantes Université, INSERM, Center for Research in Transplantation and Translational Immunology, France	Drafting/revision of the manuscript for content, including medical writing for content
Sandrine Wiertlewski, MD	CHU Nantes, Nantes Université, INSERM, Center for Research in Transplantation and Translational Immunology; CIC INSERM 1413, Nantes; CHU Nantes, Nantes Université, Service de Neurologie, Nantes, France	Drafting/revision of the manuscript for content, including medical writing for content
Pierre-Antoine Gourraud, PhD, MPH	CHU Nantes, Nantes Université, INSERM, Center for Research in Transplantation and Translational Immunology; CHU Nantes, Nantes Université, Clinique des données, Nantes, France	Drafting/revision of the manuscript for content, including medical writing for content
Laureline Berthelot, PhD	CHU Nantes, Nantes Université, INSERM, Center for Research in Transplantation and Translational Immunology, France	Drafting/revision of the manuscript for content, including medical writing for content, and study concept or design
David Laplaud, MD, PhD	CHU Nantes, Nantes Université, INSERM, Center for Research in Transplantation and Translational Immunology; CIC INSERM 1413, Nantes; CHU Nantes, Nantes Université, Service de Neurologie, Nantes, France	Drafting/revision of the manuscript for content, including medical writing for content, and study concept or design

References

1. Hauser SL, Bar-Or A, Comi G, et al. Ocrelizumab versus interferon beta-1a in relapsing multiple sclerosis. *New Engl J Med.* 2017;376(3):221-234. doi. 10.1056/NEJMoa1601277.
2. Hauser SL, Bar-Or A, Cohen JA, et al. Ofatumumab versus teriflunomide in multiple sclerosis. *N Engl J Med.* 2020;383(6):546-557. doi. 10.1056/NEJMoa1917246.
3. Granqvist M, Boremalm M, Poorghobad A, et al. Comparative effectiveness of rituximab and other initial treatment choices for multiple sclerosis. *JAMA Neurol.* 2018;75(3):320. doi. 10.1001/jamaneurol.2017.4011.
4. Harris DP, Haynes L, Sayles PC, et al. Reciprocal regulation of polarized cytokine production by effector B and T cells. *Nat Immunol.* 2000;1(6):475-482. doi. 10.1038/82717.
5. Batista FD, Harwood NE. The who, how and where of antigen presentation to B cells. *Nat Rev Immunol.* 2009;9(1):15-27. doi. 10.1038/nri2454.
6. Magliozzi R, Howell O, Vora A, et al. Meningeal B-cell follicles in secondary progressive multiple sclerosis associate with early onset of disease and severe cortical pathology. *Brain.* 2006;130(4):1089-1104. doi. 10.1093/brain/awm038.
7. Haider L, Zrzavy T, Hametner S, et al. The topograpy of demyelination and neurodegeneration in the multiple sclerosis brain. *Brain.* 2016;139(3):807-815. doi. 10.1093/brain/awv398.
8. Bar-Or A, Fawaz L, Fan B, et al. Abnormal B-cell cytokine responses a trigger of T-cell-mediated disease in MS? *Ann Neurol.* 2010;67(4):452-461. doi. 10.1002/ana.21939.
9. Jelcic I, Al Nimer F, Wang J, et al. Memory B cells activate brain-homing, autoreactive CD4+ T cells in multiple sclerosis. *Cell.* 2018;175(1):85-100.e23. doi. 10.1016/j.cell.2018.08.011.
10. Palanichamy A, Jahn S, Nickles D, et al. Rituximab efficiently depletes increased CD20-expressing T cells in multiple sclerosis patients. *J Immunol.* 2014;193(2):580-586. doi. 10.4049/jimmunol.1400118.
11. Schuh E, Berer K, Mulazzani M, et al. Features of human CD3 $^{+}$ CD20 $^{+}$ T cells. *J Immunol.* 2016;197(4):1111-1117. doi. 10.4049/jimmunol.1600089.
12. Sabatino JJ, Wilson MR, Calabresi PA, Hauser SL, Schneck JP, Zamvil SS. Anti-CD20 therapy depletes activated myelin-specific CD8 $^{+}$ T cells in multiple sclerosis. *Proc Natl Acad Sci.* 2019;116(51):25800-25807. doi. 10.1073/pnas.1915309116.
13. von Essen MR, Ammitzbøll C, Hansen RH, et al. Proinflammatory CD20+ T cells in the pathogenesis of multiple sclerosis. *Brain.* 2019;142(1):120-132. doi. 10.1093/brain/awy301.
14. Ochs J, Nissimov N, Torke S, et al. Proinflammatory CD20^{+} T cells contribute to CNS-directed autoimmunity. *Sci Transl Med.* 2022;14(638):eabi4632. doi. 10.1126/scitranslmed.abi4632.
15. von Essen MR, Hansen RH, Højgaard C, Ammitzbøll C, Wiendl H, Sellebjerg F. Ofatumumab modulates inflammatory T cell responses and migratory potential in patients with multiple sclerosis. *Neurol Neuroimmunol Neuroinflamm.* 2022;9(4):e200004. doi. 10.1212/NXI.0000000000200004.
16. Polman CH, Reingold SC, Banwell B, et al. Diagnostic criteria for multiple sclerosis: 2010 Revisions to the McDonald criteria. *Ann Neurol.* 2011;69(2):292-302. doi. 10.1002/ana.22366.
17. van Langelaar J, van der Vuurst de Vries RM, Janssen M, et al. T helper 17.1 cells associate with multiple sclerosis disease activity: perspectives for early intervention. *Brain.* 2018;141(5):1334-1349. doi. 10.1093/brain/awy069.
18. Nicol B, Salou M, Vogel I, et al. An intermediate level of CD161 expression defines a novel activated, inflammatory, and pathogenic subset of CD8+ T cells involved in multiple sclerosis. *J Autoimmun.* 2018;88:61-74. doi. 10.1016/j.jaut.2017.10.005.
19. Quendt C, Ochs J, Häusser-Kinzel S, Häusler D, Weber MS. Proinflammatory CD20 $^{+}$ T cells are differentially affected by multiple sclerosis therapeutics. *Ann Neurol.* 2021;90(5):834-839. doi. 10.1002/ana.26216.
20. Saligrama N, Zhao F, Sikora MJ, et al. Opposing T cell responses in experimental autoimmune encephalomyelitis. *Nature.* 2019;572(7770):481-487. doi. 10.1038/s41586-019-1467-x.
21. Li J, Zaslavsky M, Su Y, et al. KIR+CD8+ T cells suppress pathogenic T cells and are active in autoimmune diseases and COVID-19. *Science.* 2022;376(6590):eabi9591. doi. 10.1126/science.abi9591.
22. Herich S, Schneider-Hohendorf T, Rohlmann A, et al. Human CCRShigh effector memory cells perform CNS parenchymal immune surveillance via GZMK-mediated transendothelial diapedesis. *Brain.* 2019;142(11):3411-3427. doi. 10.1093/brain/awz301.
23. Sorce S, Myburgh R, Krause KH. The chemokine receptor CCR5 in the central nervous system. *Prog Neurobiol.* 2011;93(2):297-311. doi. 10.1016/j.pneurobio.2010.12.003.
24. Nissimov N, Hajiyeva Z, Torke S, et al. B cells reappear less mature and more activated after their anti-CD20–mediated depletion in multiple sclerosis. *Proc Natl Acad Sci USA.* 2020;117(41):25690-25699. doi. 10.1073/pnas.2012249117.
25. Fernández-Velasco JI, Kuhle J, Monreal E, et al. Effect of ocrelizumab in blood leukocytes of patients with primary progressive MS. *Neurol Neuroimmunol Neuroinflamm.* 2021;8(2):e940. doi. 10.1212/NXI.0000000000000940.
26. Sato W, Tomita A, Ichikawa D, et al. CCR2^{+} CCR5^{+} T cells produce matrix metalloproteinase-9 and osteopontin in the pathogenesis of multiple sclerosis. *J Immunol.* 2012;189(10):5057-5065. doi. 10.4049/jimmunol.1202026.
27. Mexhitaj I, Nyirenda MH, Li R, et al. Abnormal effector and regulatory T cell subsets in paediatric-onset multiple sclerosis. *Brain.* 2019;142(3):617-632. doi. 10.1093/brain/awz017.
28. Gingele S, Jacobus TL, Konen FF, et al. Ocrelizumab depletes CD20^{+} T cells in multiple sclerosis patients. *Cells.* 2018;8(1):E12. doi. 10.3390/cells8010012.
29. Lovett-Racke AE, Yang Y, Liu Y, et al. B cell depletion changes the immune cell profile in multiple sclerosis patients: one-year report. *J Neuroimmunology.* 2021;359:577676. doi. 10.1016/j.jneuroim.2021.577676.
30. Sørensen TL, Tani M, Jensen J, et al. Expression of specific chemokines and chemokine receptors in the central nervous system of multiple sclerosis patients. *J Clin Invest.* 1999;103(6):807-815. doi. 10.1172/JCI5150.
31. Karampoor S, Zahednasab H, Amini R, Esghaei M, Sholeh M, Keyvani H. Maraviroc attenuates the pathogenesis of experimental autoimmune encephalitis. *International Immunopharmacology.* 2020;80:106138. doi. 10.1016/j.intimp.2019.106138.
32. Pardridge WM. Drug transport across the blood–brain barrier. *J Cereb Blood Flow Metab.* 2012;32(11):1959-1972. doi. 10.1038/jcbfm.2012.126.

Immune Profiling Reveals the T-Cell Effect of Ocrelizumab in Early Relapsing-Remitting Multiple Sclerosis

Alexandra Garcia, Emilie Dugast, Sita Shah, et al.

Neurol Neuroimmunol Neuroinflamm 2023;10;
DOI 10.1212/NXI.0000000000200091